Original Article

Dosimetry of indigenously developed ^{192}Ir high-dose rate brachytherapy source: An EGSnrc Monte Carlo study

Sridhar Sahoo, T. Palani Selvam, S. D. Sharma, Trupti Das[1], A. C. Dey[1], B. N. Patil[1], K. V. S. Sastri[1]

Radiological Physics and Advisory Division, Bhabha Atomic Research Centre, [1]Board of Radiation Isotope and Technology, Vashi, Navi Mumbai, Maharashtra, India

Received on: 01-12-2015 Review completed on: 12-01-2016 Accepted on: 12-01-2016

ABSTRACT

Clinical application using high-dose rate (HDR) ^{192}Ir sources in remote afterloading technique is a well-established treatment method. In this direction, Board of Radiation and Isotope Technology (BRIT) and Bhabha Atomic Research Centre, India, jointly indigenously developed a remote afterloading machine and ^{192}Ir HDR source. The two-dimensional (2D) dose distribution and dosimetric parameters of the BRIT ^{192}Ir HDR source are generated using EGSnrc Monte Carlo code system in a 40 cm dia × 40 cm height cylindrical water phantom. The values of air-kerma strength and dose rate constant for BRIT ^{192}Ir HDR source are $9.894 \times 10^{-8} \pm 0.06\%$ UBq^{-1} and $1.112 \pm 0.11\%$ $cGyh^{-1}U^{-1}$, respectively. The values of radial dose function ($g_L(r)$) of this source compare well with the corresponding values of BEBIG, Flexisource, and GammaMed 12i source models. This is because of identical active lengths of the sources (3.5 mm) and the comparable phantom dimensions. A comparison of $g_L(r)$ values of BRIT source with microSelectron-v1 show differences about 2% at r = 6 cm and up to 13% at r = 12 cm, which is due to differences in phantom dimensions involved in the calculations. The anisotropy function of BRIT ^{192}Ir HDR source is comparable with the corresponding values of microSelectron-v1 (classic) HDR source.

Key words: Brachytherapy; ^{192}Ir high-dose rate source; TG43; EGSnrc Monte Carlo

Introduction

In brachytherapy, sealed radioactive sources are placed near or inside a tumor, to deliver prescribed radiation dose to tumor by intracavitary, interstitial, or surface mold technique. In this treatment modality, a high radiation dose can be delivered locally to the tumor with rapid dose falloff in the surrounding normal tissue.

Address for correspondence:
Mr. Sridhar Sahoo,
Radiological Physics and Advisory Division, Bhabha Atomic Research Centre, Room No. 204, CT and CRS Building, Anushaktinagar, Mumbai - 400 094. Maharashtra, India.
E-mail: barcsridhar@gmail.com

Access this article online	
Quick Response Code:	Website: www.jmp.org.in
	DOI: 10.4103/0971-6203.181639

^{192}Ir high-dose rate (HDR) sources are widely used in brachytherapy treatment because of remote afterloading technology that reduces exposure to hospital personnel, high source activity, higher dose rate, short treatment time, and more important is comfort to patient. Many HDR ^{192}Ir source models such as microSelectron-v1 (classic), microSelectron-v2, BEBIG GmBH, VariSource (classic), VariSource (VS2000), Flexisource, and GammaMed 12i are available worldwide for clinical applications.[1-7]

Board of Radiation and Isotope Technology (BRIT) and Bhabha Atomic Research Centre (BARC) jointly developed a remote afterloading HDR machine (Karknidon) for brachytherapy treatments. Seven machines have been already

This is an open access article distributed under the terms of the Creative Commons Attribution-NonCommercial-ShareAlike 3.0 License, which allows others to remix, tweak, and build upon the work non-commercially, as long as the author is credited and the new creations are licensed under the identical terms.

For reprints contact: reprints@medknow.com

How to cite this article: Sahoo S, Selvam TP, Sharma SD, Das T, Dey AC, Patil BN, *et al.* Dosimetry of indigenously developed ^{192}Ir high-dose rate brachytherapy source: An EGSnrc Monte Carlo study. J Med Phys 2016;41:115-22.

been fabricated, which underwent several tests involving a dummy source. Performance of these machines is found to be satisfactory. This machine will utilize indigenously developed ^{192}Ir HDR source. Two such prototype active sources have been indigenously made recently by BRIT and BARC, to standardize methodology of active core fabrication inside a hot cell using a remote controlled laser welding equipment. Active sources are yet to be loaded in the HDR treatment units.

Table 1 compares the source geometries, which includes encapsulation material/thickness and distal, and proximal end thicknesses of different ^{192}Ir HDR sources including BRIT ^{192}Ir HDR source, including the details of cable length modeled in the Monte Carlo calculations. The proximal and distal end thickness of BRIT ^{192}Ir HDR source is different from the other HDR source models.

A study published by Li *et al.*[8] provides recommendations on dosimetric prerequisites for routine clinical use of photon emitting brachytherapy sources with average energy higher than 50 keV. As per the recommendations, for commercially distributed sources, single source-based dose distribution used for clinical treatment planning should be based on two dose-rate determinations, one of which is theoretical method such as Monte Carlo method and the other an experimental measurement. However, for conventionally encapsulated ^{192}Ir sources similar in design to existing ones, a single dosimetric study either Monte Carlo simulation techniques, or other transport equation solutions, or experimental dosimetry methods is sufficient.[8,9]

The objective of this work is to calculate American Association of Physicists in Medicine (AAPM) TG-43 dosimetry parameters and dose distribution in liquid water for the BRIT ^{192}Ir HDR source and utilize the same for the indigenous development of treatment planning software.[10,11] DOSRZnrc and FLURZnrc user-codes[12] of the EGSnrc Monte Carlo code system[13] are used for this purpose. The calculated dosimetry parameters are compared with published results of other ^{192}Ir HDR sources.[1-7]

Materials and Methods

In this ^{192}Ir HDR source, the radioactive material is in the form of ^{192}Ir slugs of 0.6-mm-dia × 3.5-mm-length. The active source is encapsulated in stainless steel-316L capsule of thickness 0.2 mm, which is welded remotely by argon gas laser welding process. The distal end of the capsule is spherical in shape with radius of 0.55 mm and length of the proximal end is 2 mm. The total length of the capsule is 6 mm and diameter is 1.1 mm. A schematic diagram of the BRIT ^{192}Ir HDR source is shown in Figure 1a.

Monte Carlo calculations

DOSRZnrc user-code[12] of the EGSnrc Monte Carlo code system[13] is used for modeling of the BRIT ^{192}Ir HDR source in liquid water. The DOSRZnrc user-code[12] calculates absorbed dose and kerma in cylindrical regions in an RZ cylindrical geometry. The material, mass density, and geometric details of the source needed for simulations

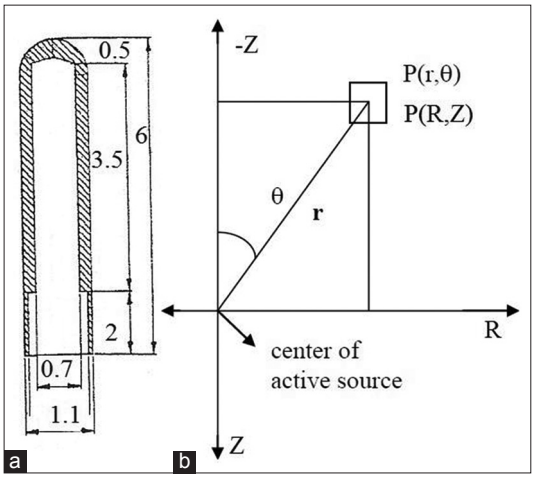

Figure 1: Schematic diagram of the Board of Radiation and Isotope Technology ^{192}Ir high-dose rate source simulated in the EGSnrc Monte Carlo code. Dimensions shown are in millimeters (not to scale). (b) The cartesian coordinate system, P(*R*,*Z*) used in the EGSnrc simulations. The coordinate of *P* will be (*r*,θ) in polar coordinate system. The origin of the coordinate system is chosen at the center of the active source

Table 1: Comparison of source designs, encapsulation material/thickness and cable length modeled in Monte Carlo calculations of different ^{192}Ir high-dose rate sources

Source model	*Active length*	*Active diameter*	*Total length*	*Total diameter*	*Encapsulation material and thickness*	*Distal end thickness*	*Proximal end thickness + cable length in the simulation*	*DRC ($cGyh^{-1}U^{-1}$)*	*DRC/G (1, 90^0) ($cGyh^{-1}U^{-1}$ cm^2)*
BRIT ^{192}Ir HDR	3.5	0.6	6	1.1	SS316L, 0.2	0.5	2+1	1.112	1.123
BEBIG GmbH[3]	3.5	0.6	4.9	1	SS316L, 0.15	0.84	0.55*	1.108	1.119
Flexisource[6]	3.5	0.6	4.6	0.85	SS304	0.65	0.45+5	1.109	1.120
microSelectron-v1[1]	3.5	0.6	5	1.1	SS304, 0.2	0.35	1.15+1.85	1.115	1.126
VariSource-classic[4]	10	0.35		0.61	Ni/Ti alloy	1	3*	1.044	1.126
microSelectron-v2[2]	3.6	0.65	4.5	0.9	SS316L, 0.1	0.2	0.70+2	1.108	1.120
VariSource-VS2000[5]	5	0.34		0.61	Ni/Ti wire	1	*	1.101	1.123
GammaMed 12i[7]	3.5	0.6	4.96	1.1	SS316L, 0.2	0.86	0.5+60	1.118	1.129

All dimensions are in mm. Also presented in the table are values of DRC. *Cable length in the simulation is not reported. BRIT: Board of Radiation and Isotope Technology, HDR: High-dose rate, DRC: Dose rate constant

are taken from source supplier. Figure 1b shows the coordinate system used in the DOSRZnrc simulations. In the Monte Carlo calculations, the source is immersed in a 40 cm dia × 40 cm height cylindrical water phantom to get full scatter conditions up to a distance of 20 cm from the source.[14] The density of water was taken as 0.998 gcm^{-3} at 22°C, consistent with AAPM TG-43U1 formalism.[11] A grid system was simulated with thin cylindrical shells of different thickness (δR, δZ) around source axis where δR represents radial distance and δZ represents axial distance. The thickness of shells, δR = δZ is 0.5 mm (up to R=Z=5 cm), 1 mm (up to R=Z=10 cm), and 2 mm (up to R=Z=14 cm). The photon energy spectrum of the ^{192}Ir source is taken from literature.[14]

The origin of the coordinate system is chosen at the geometric center of the active core. In the simulation, we modeled 1 mm long stainless steel-316L cable at proximal end of the source. The distal end of the source is a rounded tip of 0.5-mm-thickness and 0.55-mm-radius, which cannot be simulated in DOSRZnrc code. The thickness part (0.5 mm) is divided into 10 slabs each of thickness 0.05 mm and the radius (0.55 mm) is divided into 11 cylinders each of radius 0.055 mm. This geometrical modeling makes a step-like shape, which tries to mimic the real rounded tip.

The geometry factor, $G(r,\theta)$ accounts for the distribution of radioactivity in the active source volume, which is calculated either by point or line source approximation. TG-43U1 report recommends the use of line source based geometry factors for evaluation of 2D dose distributions. This approximation is suitable for dose estimation at larger distances from the source. However, this approximation introduces errors up to 3% at radial distances close to the sources.[15] Therefore, we have calculated the exact geometry factor, up to 1 cm distances around the source. The difference of 0.8% at 0.2 cm and 0.3% at 0.5 cm along transverse axis is observed between exact and line source based geometry factor.

The dose value for a particular location in polar coordinate (r,θ) is estimated by converting the polar coordinate into corresponding cartesian coordinate (R, Z). When this coordinate (R, Z) is not falling with in the centre of voxel, dose is estimated from dose values of four nearest points, (R_1, Z_1), (R_2, Z_2), (R_3, Z_3), and (R_4, Z_4) using bilinear interpolation. Accuracy of the interpolation is improved by dividing the dose values with the exact geometry function, up to a distance of 1 cm from the active center of the source and line source-based geometry function thereafter. These dose values in polar coordinate are used to estimate anisotropy function for this source. The above-described interpolation approach has been also applied elsewhere.[16,17]

The air-kerma strength, S_k of the source is defined as the product of air-kerma rate at distance, in free space, measured along the transverse bisector of the source and the square of the distance.[11] In the study, air-kerma strength per Bq (U/Bq) is calculated for the BRIT ^{192}Ir source using the FLURZnrc code.[12] In this calculation, the source was in vacuum. This is consistent with the updated TG-43U1 formalism. As detailed secondary electrons transport is not important, ECUT = 1 MeV (kinetic energy) is set in the FLURZnrc simulations. The photon fluence energy spectrum in 10 keV interval, along the transverse axis, at 100 cm is scored and subsequently converted into air-kerma per initial photon, k_{air} (Gy/initial photon) using the mass-energy-absorption coefficient of air.[18] The composition of air considered is as recommended by the TG-43U1 protocol (40% humidity).[11] The k_{air} values were then converted to S_k per unit activity (cGycm^{2}h^{-1}Bq^{-1} or UBq^{-1}).

The PEGS4 dataset needed for the above calculations is based on XCOM compilations.[19] We set AE = 521 keV and AP = 10 keV while creating PEGS4 dataset, where the parameters AP and AE are the low-energy threshold for the production of secondary bremsstrahlung photons and knock-on electrons. All DOSRZnrc simulations utilize the PRESTA-II electron step length and EXACT boundary-crossing algorithms. The electron step size parameter is ESTEP set to 0.25. To increase the speed of the calculations, for all simulations, electron range rejection technique is used by setting ESAVE = 2 MeV. The value of photon transport cutoff parameter PCUT used in all simulations is 10 keV. The value of ECUT used in absorbed dose calculations is 521 keV.

Up to 2 × 10^9 primary photon histories are simulated. All Monte Carlo simulations were run on a 32-bit Intel (R) Core i3, 3.2 GHz computer. The statistical uncertainties on the calculated estimates have a coverage factor k = 1. The uncertainties on the dose values varies between 0.1% and 1% for the regions up to Z = 2 cm, R = 0.2–14 cm. For regions Z = 2–5 cm and R = 0.2–0.5 cm, the uncertainties varied between 1% and 2%. For regions Z = 5–15 cm and R = 0.2–0.5 cm, the uncertainties varied between 2% and 3%. The uncertainty on air-kerma calculation is <0.10%.

Results and Discussion

Two-dimensional dose rate distribution

Absorbed dose per unit air-kerma strength (in cGyh^{-1}U^{-1}) is presented along both axial and radial distances up to 14 cm from the centre of the active source in Table 2.

Dose rate constant, Λ

The value of air-kerma strength is 9.894 × 10^{-8} ± 0.06% UBq^{-1}. The calculated value of Λ for BRIT ^{192}Ir HDR source is 1.112 ± 0.11% cGyh^{-1}U^{-1} and is in excellent agreement with the published values of Λ for other ^{192}Ir HDR source

Table 2: Dose rate per unit air-kerma strength (cGyh^{-1}U^{-1}) around the Board of Radiation and Isotope Technology ^{192}Ir high-dose rate source in a 40 cm diameter x 40 cm height cylindrical liquid water phantom of density 0.998 g/cm^3

Distance along, Z (cm)	*Distance away, r (cm)*																				
	0	*0.2*	*0.3*	*0.5*	*0.75*	*1*	*1.5*	*2*	*2.5*	*3*	*3.5*	*4*	*4.5*	*5*	*6*	*7*	*8*	*9*	*10*	*12*	*14*
−14	0.00377	0.00381	0.00381	0.00380	0.00384	0.00391	0.00389	0.00388	0.00387	0.00388	0.00383	0.00376	0.00370	0.00367	0.00348	0.00325	0.00306	0.00281	0.00258	0.00212	0.00171
−12	0.00538	0.00542	0.00534	0.00543	0.00556	0.00552	0.00556	0.00555	0.00566	0.00557	0.00549	0.00545	0.00534	0.00520	0.00486	0.00452	0.00415	0.00378	0.00341	0.00275	0.00215
−10	0.00798	0.00825	0.00818	0.00827	0.00832	0.00844	0.00839	0.00849	0.00848	0.00828	0.00822	0.00803	0.00774	0.00750	0.00691	0.00626	0.00565	0.00504	0.00445	0.00346	0.00264
−8	0.0127	0.0131	0.0127	0.0133	0.0133	0.0133	0.0137	0.0135	0.0135	0.0132	0.0128	0.0122	0.0117	0.0112	0.00994	0.00875	0.00765	0.00663	0.00576	0.00429	0.00319
−7	0.0164	0.0170	0.0170	0.0172	0.0175	0.0177	0.0179	0.0178	0.0176	0.0170	0.0163	0.0156	0.0147	0.0138	0.0120	0.0103	0.00887	0.00759	0.00648	0.00472	0.00345
−6	0.0222	0.0223	0.0228	0.0233	0.0236	0.0240	0.0243	0.0244	0.0235	0.0225	0.0213	0.0199	0.0185	0.0171	0.0145	0.0122	0.0103	0.00864	0.00724	0.00517	0.00373
−5	0.0313	0.0324	0.0330	0.0339	0.0345	0.0348	0.0352	0.0345	0.0325	0.0307	0.0281	0.0259	0.0235	0.0213	0.0175	0.0143	0.0117	0.00963	0.00800	0.00561	0.00397
−4.5	0.0386	0.0397	0.0408	0.0415	0.0419	0.0431	0.0432	0.0415	0.0391	0.0358	0.0327	0.0295	0.0265	0.0238	0.0191	0.0154	0.0124	0.0102	0.00841	0.00583	0.00409
−4	0.0478	0.0500	0.0503	0.0520	0.0535	0.0545	0.0543	0.0511	0.0472	0.0425	0.0381	0.0337	0.0299	0.0266	0.0208	0.0165	0.0132	0.0107	0.00879	0.00602	0.00420
−3.5	0.0614	0.0642	0.0656	0.0690	0.0703	0.0713	0.0690	0.0640	0.0576	0.0507	0.0442	0.0387	0.0337	0.0294	0.0226	0.0176	0.0140	0.0112	0.00915	0.00619	0.00430
−3	0.0822	0.0871	0.0901	0.0929	0.0959	0.0959	0.0908	0.0810	0.0707	0.0605	0.0518	0.044	0.0376	0.0325	0.0243	0.0187	0.0147	0.0117	0.00944	0.00635	0.00441
−2.5	0.118	0.125	0.128	0.135	0.138	0.136	0.123	0.105	0.0870	0.0720	0.0597	0.0497	0.0420	0.0354	0.0261	0.0197	0.0153	0.0121	0.00974	0.00650	0.00444
−2	0.180	0.196	0.205	0.213	0.213	0.203	0.170	0.136	0.108	0.0857	0.0686	0.0557	0.0461	0.0384	0.0277	0.0207	0.0159	0.0125	0.00998	0.00665	0.00453
−1.5	0.318	0.355	0.370	0.379	0.361	0.323	0.241	0.177	0.131	0.0996	0.0774	0.0617	0.0498	0.0410	0.0290	0.0215	0.0163	0.0128	0.0102	0.00670	0.00458
−1	0.724	0.836	0.858	0.814	0.682	0.543	0.341	0.223	0.155	0.113	0.0851	0.0662	0.0531	0.0431	0.0300	0.0220	0.0167	0.0130	0.0103	0.00679	0.00465
−0.75	1.335	1.548	1.532	1.306	0.967	0.704	0.396	0.246	0.165	0.118	0.0883	0.0682	0.0542	0.0439	0.0305	0.0223	0.0168	0.0131	0.0103	0.00681	0.00464
−0.5	3.373	3.632	3.191	2.192	1.358	0.889	0.448	0.264	0.174	0.122	0.0903	0.0694	0.0551	0.0445	0.0306	0.0224	0.0169	0.0131	0.0103	0.00682	0.00464
−0.25	27.0159	11.730	7.367	3.514	1.766	1.047	0.485	0.277	0.179	0.125	0.0919	0.0703	0.0555	0.0450	0.0309	0.0225	0.0169	0.0131	0.0104	0.00679	0.00463
0	-	22.862	11.232	4.308	1.960	1.112	0.498	0.281	0.181	0.125	0.0922	0.0705	0.0557	0.0450	0.0310	0.0225	0.0170	0.0132	0.0104	0.00688	0.00467
0.25	-	11.740	7.357	3.514	1.766	1.0452	0.484	0.277	0.178	0.125	0.0917	0.0705	0.0556	0.0448	0.0309	0.0224	0.0169	0.0131	0.0104	0.00684	0.00465
0.5	3.019	3.619	3.183	2.191	1.358	0.886	0.448	0.264	0.174	0.122	0.0905	0.0695	0.0549	0.0444	0.0307	0.0224	0.0169	0.0131	0.0104	0.00683	0.00464
0.75	1.172	1.517	1.525	1.300	0.966	0.705	0.396	0.246	0.165	0.118	0.0881	0.068	0.0539	0.0441	0.0305	0.0222	0.0168	0.0131	0.0103	0.00679	0.00464
1	0.639	0.803	0.845	0.812	0.680	0.543	0.340	0.224	0.155	0.113	0.0854	0.0664	0.0528	0.0431	0.0301	0.0220	0.0167	0.0130	0.0103	0.00676	0.00463
1.5	0.282	0.325	0.356	0.376	0.358	0.323	0.242	0.177	0.131	0.0995	0.0775	0.0614	0.0499	0.0411	0.0290	0.0215	0.0163	0.0128	0.0101	0.00669	0.00459
2	0.161	0.177	0.189	0.209	0.212	0.202	0.170	0.136	0.107	0.0853	0.0686	0.0559	0.0460	0.0385	0.0277	0.0207	0.0158	0.0124	0.00993	0.00661	0.00457
2.5	0.105	0.112	0.119	0.130	0.135	0.135	0.123	0.104	0.0872	0.0721	0.0598	0.0500	0.0419	0.0355	0.0261	0.0197	0.0153	0.0121	0.00973	0.00648	0.00445
3	0.075	0.0786	0.0816	0.0884	0.0942	0.0954	0.0901	0.0811	0.0701	0.0605	0.0514	0.0441	0.0377	0.0324	0.0244	0.0187	0.0146	0.0117	0.00942	0.00636	0.00439
3.5	0.0564	0.0583	0.0603	0.0643	0.0685	0.0698	0.0689	0.0637	0.0570	0.0506	0.0443	0.0386	0.0336	0.0294	0.0226	0.0176	0.0140	0.0112	0.00909	0.00619	0.00430
4	0.0439	0.0452	0.0460	0.0492	0.0514	0.0537	0.0535	0.0507	0.0472	0.0425	0.0379	0.0338	0.0298	0.0264	0.0208	0.0165	0.0132	0.0107	0.00873	0.00601	0.00422
4.5	0.0352	0.0365	0.0369	0.0386	0.0404	0.0423	0.0425	0.0414	0.0390	0.0362	0.0326	0.0296	0.0266	0.0238	0.0192	0.0154	0.0125	0.0102	0.00841	0.00578	0.00411
5	0.0289	0.0302	0.0302	0.0311	0.0324	0.0338	0.0345	0.0340	0.0324	0.0305	0.0281	0.0257	0.0235	0.0214	0.0174	0.0143	0.0117	0.00967	0.00802	0.00560	0.00398
6	0.0208	0.0215	0.0213	0.0218	0.0226	0.0231	0.0240	0.0240	0.0234	0.0224	0.0212	0.02	0.0185	0.0170	0.0145	0.0122	0.0102	0.00858	0.00724	0.00517	0.00373
7	0.0154	0.0158	0.0162	0.0158	0.0164	0.0169	0.0175	0.0175	0.0174	0.0170	0.0162	0.0155	0.0146	0.0137	0.0119	0.0103	0.00885	0.00756	0.00646	0.00473	0.00344
8	0.0118	0.0124	0.0121	0.0124	0.0123	0.0129	0.0132	0.0133	0.0132	0.0130	0.0128	0.0123	0.0116	0.0111	0.00993	0.00875	0.00765	0.00664	0.00576	0.00428	0.00318
10	0.00765	0.00744	0.00778	0.00777	0.00786	0.00793	0.00803	0.00821	0.00813	0.00821	0.00812	0.00795	0.00771	0.00744	0.00688	0.00623	0.00565	0.00505	0.00445	0.00345	0.00265
12	0.00518	0.00519	0.0052	0.00541	0.00516	0.00537	0.00546	0.00546	0.00557	0.00545	0.00544	0.00537	0.00528	0.00518	0.00484	0.00450	0.00415	0.00375	0.00340	0.00274	0.00215
14	0.00362	0.00361	0.00377	0.00378	0.00374	0.00370	0.00377	0.00378	0.00378	0.00381	0.00374	0.00372	0.00368	0.00367	0.00347	0.00326	0.00302	0.00280	0.00258	0.00212	0.00171

The positive Z-axis is toward the proximal end. The origin is taken at the active center of the source

models [Table 1] other than VariSource (classic). This is due to same active length (3.5 mm) of the ^{192}Ir HDR sources.

The value of Λ for BRIT ^{192}Ir HDR source is higher by 6.5% when compared to VariSource (classic).[4] This is because the active length of VariSource (classic) is 1 cm. For a given radionuclide, the main influencing factor which affects Λ is the geometry factor. The values of Λ when corrected for geometry factor are comparable [Table 1].

Radial dose function

The values of $g_L(r)$ for BRIT ^{192}Ir HDR source calculated for distances r = 0.25–20 cm are presented in Table 3. Figure 2 compares the plot of $g_L(r)$ with distance for different HDR ^{192}Ir sources. The $g_L(r)$ values of BRIT ^{192}Ir HDR source are almost same with that of the BEBIG, Flexisource, and GammaMed 12i source models. This is due to similar active lengths and comparable phantom dimensions used in the calculations. The 40 cm diameter × and 40 cm height cylindrical water phantom is simulated for BRIT ^{192}Ir HDR and GammaMed 12i sources whereas BEBIG and Flexisource models utilized 40 cm radius spherical water phantom. Granero *et al*. observed 1% difference in $g_L(r)$ values, for ^{192}Ir point source, at r = 10 cm, between an unbounded spherical phantom of 40 cm in radius and cylindrical phantom of 40 cm in diameter and 40 cm in height.[20]

Table 3: Radial dose function for the Board of Radiation and Isotope Technology ^{192}Ir high-dose rate source

Distance, r (cm)	*g (r)*
0.25	0.993
0.3	0.993
0.4	0.995
0.5	0.995
0.6	0.996
0.75	0.998
0.8	0.998
0.9	0.999
1	1.000
1.5	1.004
2	1.006
2.5	1.007
3	1.009
3.5	1.010
4	1.008
4.5	1.015
5	1.004
6	0.999
7	0.988
8	0.977
9	0.960
10	0.945
12	0.902
15	0.828
20	0.688

The $g_L(r)$ values for the source models such as VariSource (classic, and VS2000), microSelectron (vl-classic and v2) models are based on 30 cm dia spherical water phantom. Hence, the values of $g_L(r)$ fall rapidly for these models as compared to BRIT source model, due to lack of back scattering of photons. A comparison of $g_L(r)$ values of BRIT and source models of VariSource and microSelectron shows differences by about 2% at r = 6 cm and up to 13% at r = 12 cm.

Anisotropy function

The anisotropy function, $F(r,\theta)$ data, at radial distances r = 0.25–10 cm, at polar angles θ = 0°–180° relative to long axis of the source are presented in Table 4. Figure 3 presents the plot of $F(r,\theta)$ of the BRIT ^{192}Ir HDR source for radial distance 1 cm. The ratio of $F(r,\theta)$ of the other HDR sources to the BRIT ^{192}Ir HDR source is plotted for radial distance 5 cm, in Figure 4.

It is observed from the Figure 4 that for polar angles from 20° to 140°, $F(r,\theta)$ values are nearly independent of r and similar for all HDR sources. However, at polar angles close to the longitudinal axis of the source, (0°–20° and 140°–180°), i.e. proximal and distal end of the source, greater differences in $F(r,\theta)$ values are observed. This is mainly due to the different encapsulation thickness at proximal and distal end of the source.

Due to similar design, $F(r,\theta)$ values of BRIT ^{192}Ir HDR source and microSelectron-v1 (classic) source are comparable. Small difference in the distal end thickness of

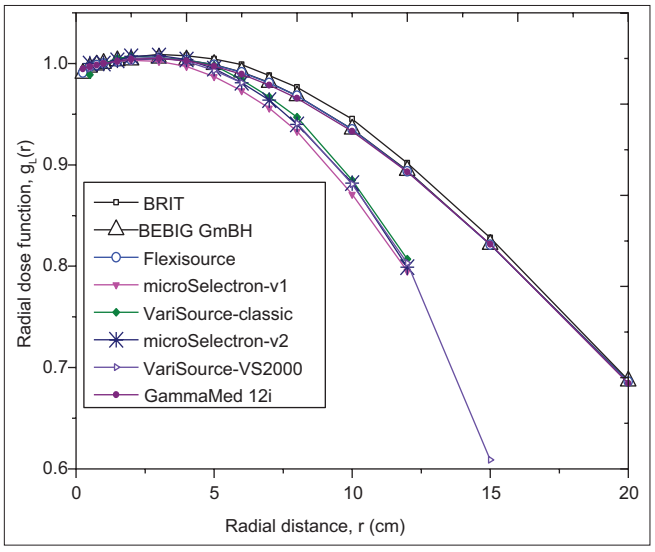

Figure 2: Comparison of the radial dose functions of various ^{192}Ir high-dose rate sources

Table 4: Anisotropy function, F (r, θ) of the Board of Radiation and Isotope Technology ^{192}Ir high-dose rate source calculated in a 40 cm diameter × 40 cm height cylindrical liquid water phantom of density 0.998 g/cm^3

	r (cm)												
θ (°)	*0.25*	*0.5*	*0.75*	*1*	*1.5*	*2*	*3*	*4*	*5*	*6*	*7*	*8*	*10*
0	0.774	0.662	0.636	0.627	0.628	0.634	0.654	0.673	0.695	0.723	0.733	0.739	0.783
1	0.783	0.662	0.636	0.628	0.625	0.635	0.660	0.691	0.702	0.731	0.739	0.751	0.768
2	0.773	0.663	0.636	0.634	0.638	0.658	0.678	0.695	0.714	0.737	0.750	0.758	0.780
3	0.770	0.662	0.638	0.642	0.652	0.664	0.687	0.703	0.724	0.743	0.755	0.758	0.795
4	0.769	0.664	0.652	0.655	0.661	0.675	0.697	0.715	0.733	0.749	0.761	0.772	0.793
5	0.774	0.676	0.666	0.669	0.677	0.687	0.710	0.726	0.743	0.757	0.770	0.776	0.801
6	0.771	0.688	0.679	0.682	0.687	0.698	0.717	0.734	0.751	0.762	0.779	0.785	0.803
7	0.772	0.699	0.691	0.699	0.700	0.712	0.732	0.744	0.761	0.770	0.793	0.795	0.818
8	0.777	0.713	0.704	0.707	0.714	0.723	0.741	0.752	0.775	0.782	0.799	0.802	0.822
9	0.793	0.726	0.717	0.718	0.725	0.734	0.753	0.763	0.781	0.791	0.802	0.812	0.829
10	0.799	0.737	0.730	0.733	0.739	0.748	0.767	0.779	0.790	0.801	0.811	0.821	0.833
12	0.820	0.762	0.758	0.759	0.766	0.773	0.787	0.798	0.809	0.820	0.839	0.838	0.852
15	0.845	0.797	0.790	0.795	0.798	0.806	0.818	0.826	0.838	0.841	0.856	0.858	0.874
20	0.886	0.845	0.842	0.840	0.845	0.848	0.857	0.866	0.872	0.878	0.885	0.885	0.897
25	0.917	0.883	0.879	0.881	0.882	0.882	0.891	0.894	0.899	0.907	0.911	0.908	0.920
30	0.937	0.910	0.907	0.908	0.907	0.910	0.915	0.918	0.922	0.927	0.931	0.927	0.930
35	0.952	0.929	0.926	0.927	0.929	0.931	0.931	0.935	0.940	0.938	0.945	0.943	0.947
40	0.964	0.947	0.953	0.947	0.946	0.946	0.949	0.952	0.954	0.955	0.956	0.951	0.957
45	0.972	0.960	0.959	0.959	0.958	0.960	0.962	0.963	0.964	0.967	0.968	0.965	0.969
50	0.978	0.972	0.971	0.971	0.972	0.971	0.973	0.974	0.974	0.975	0.977	0.974	0.976
55	0.985	0.976	0.975	0.979	0.978	0.980	0.981	0.982	0.982	0.981	0.987	0.982	0.982
60	0.989	0.983	0.981	0.984	0.986	0.986	0.985	0.985	0.986	0.986	0.992	0.984	0.984
65	0.993	0.989	0.989	0.989	0.998	0.989	0.988	0.989	0.990	0.990	0.995	0.987	0.990
70	0.995	0.992	0.992	0.995	0.994	0.995	0.994	0.996	0.994	0.994	1.001	0.992	0.995
75	0.997	0.995	0.995	0.997	0.997	0.997	0.998	0.997	0.999	0.998	1.001	0.993	0.993
80	1.001	0.997	0.998	0.999	0.998	0.998	0.999	1.002	1.002	1.000	1.000	1.000	0.999
85	1.003	1.001	0.999	1.001	1.000	1.002	1.002	0.999	0.999	0.999	1.003	0.998	1.001
90	1.000	1.000	1.000	1.000	1.000	1.000	1.000	1.000	1.000	1.000	1.000	1.000	1.000
95	1.000	1.000	0.999	1.001	1.002	1.001	0.999	1.000	1.000	0.999	1.004	1.000	1.001
100	0.998	0.996	0.997	1.000	0.999	0.998	0.997	0.998	0.998	1.000	0.999	0.997	0.998
105	0.998	0.998	0.999	0.999	0.998	0.998	0.995	0.995	0.996	0.996	0.997	0.996	0.999
110	0.995	0.993	0.993	0.998	0.993	0.996	0.996	0.995	0.995	0.993	0.998	0.990	0.993
115	0.992	0.990	0.988	0.992	0.989	0.991	0.995	0.987	0.993	0.988	0.994	0.991	0.991
120	0.991	0.984	0.983	0.986	0.984	0.987	0.987	0.985	0.985	0.984	0.990	0.983	0.990
125	0.985	0.980	0.978	0.981	0.980	0.980	0.979	0.979	0.982	0.982	0.982	0.980	0.981
130	0.981	0.970	0.969	0.972	0.969	0.971	0.972	0.971	0.973	0.975	0.976	0.970	0.975
135	0.975	0.962	0.957	0.960	0.959	0.960	0.962	0.960	0.965	0.963	0.969	0.962	0.969
140	0.965	0.949	0.945	0.948	0.946	0.948	0.948	0.958	0.952	0.952	0.960	0.955	0.962
145	0.953	0.933	0.929	0.929	0.930	0.930	0.932	0.933	0.937	0.939	0.943	0.941	0.947
150	0.940	0.910	0.905	0.907	0.905	0.908	0.911	0.914	0.917	0.922	0.925	0.923	0.939
155	0.920	0.881	0.875	0.876	0.876	0.882	0.885	0.888	0.896	0.898	0.902	0.909	0.917
160	0.892	0.845	0.836	0.835	0.840	0.841	0.848	0.855	0.864	0.873	0.875	0.879	0.893
165	0.844	0.792	0.781	0.778	0.785	0.788	0.799	0.810	0.821	0.832	0.838	0.844	0.858
168	-	0.739	0.730	0.731	0.737	0.746	0.761	0.770	0.785	0.800	0.808	0.820	0.835
170	-	0.701	0.687	0.693	0.698	0.709	0.725	0.742	0.757	0.772	0.783	0.795	0.822
171	-	0.679	0.664	0.671	0.678	0.690	0.711	0.725	0.744	0.760	0.776	0.782	0.800
172	-	0.650	0.641	0.648	0.656	0.670	0.689	0.713	0.730	0.747	0.756	0.772	0.789
173	-	0.621	0.614	0.624	0.634	0.652	0.673	0.697	0.714	0.737	0.747	0.754	0.783
174	-	0.606	0.595	0.601	0.613	0.628	0.654	0.678	0.698	0.720	0.735	0.747	0.778
175	-	0.598	0.582	0.585	0.597	0.612	0.640	0.663	0.686	0.714	0.723	0.742	0.773
176	-	0.585	0.569	0.574	0.580	0.597	0.627	0.650	0.676	0.699	0.708	0.727	0.757
177	-	0.585	0.560	0.564	0.571	0.588	0.620	0.641	0.667	0.688	0.703	0.712	0.742

Contd...

Table 4: Contd...

		r (cm)											
178	-	0.586	0.555	0.554	0.560	0.576	0.605	0.634	0.660	0.682	0.693	0.711	0.740
179	-	0.585	0.557	0.553	0.554	0.567	0.595	0.623	0.648	0.676	0.678	0.701	0.733
180	-	0.586	0.559	0.549	0.556	0.568	0.597	0.616	0.646	0.671	0.680	0.689	0.728

The origin is taken at the active centre of the source and the origin of the polar angle is at the tip side (distal end) of the source

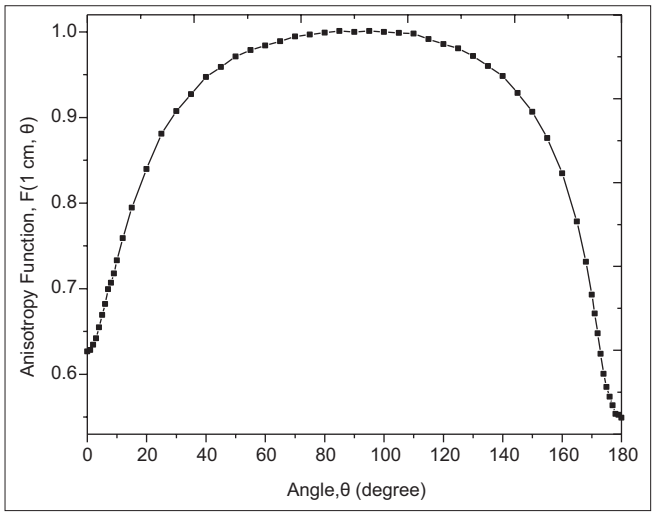

Figure 3: Anisotropy function of Board of Radiation and Isotope Technology ^{192}Ir high-dose rate source for radial distance *r* = 1 cm

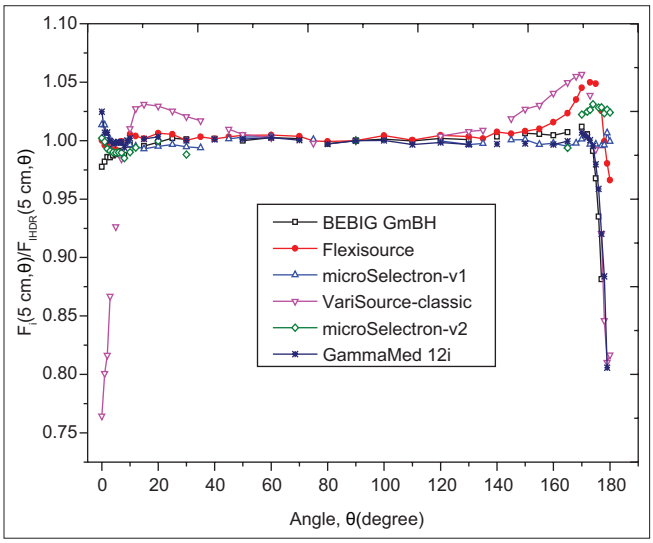

Figure 4: Ratio of anisotropy function of ^{192}Ir clinical sources with Board of Radiation and Isotope Technology ^{192}Ir high-dose rate source for radial distance *r* = 5 cm

these sources did not show observable differences in the anisotropy.

The F(r,θ) values of BRIT source compares well with microSelectron-v2 source for θ = 0°–165° and for angles >165° significant differences up to 6% are observed. The microSelectron-v2 source shows more anisotropy than BRIT source. This is due to differences in the geometry in the proximal end.

The VariSource (classic) source shows more anisotropy due to its longer active length (10 mm). Anisotropy is 30% higher than BRIT source along source axis for *r* = 1 cm.

A difference of about 5% at *r* = 1 cm and 2% at *r* = 5, 10 cm, in F(*r*,θ) values along distal end (θ = 0°) are observed between BRIT and BEBIG source. This is due to difference in distal end thickness, which is 0.5 mm for BRIT source and 0.84 mm for BEBIG source. Similarly, significant differences up to 20% along proximal end are observed between two sources, which is also due to the difference in end thickness.

A significant difference of up to 15% along proximal end is observed between BRIT and Flexisource models. This is due to 0.45 mm end thickness and 5 mm steel cable considered in the Flexisource simulations. A difference of up to 20% along proximal end is also observed between BRIT and GammaMed 12i source models as the later source utilized 0.5 mm end thickness and 60 mm stainless steel cable in the Monte Carlo calculations.

Conclusions

The AAPM TG-43 dosimetric parameters of the BRIT ^{192}Ir HDR source are generated using the EGSnrc Monte Carlo code system. The calculated dose rate constant of BRIT ^{192}Ir HDR source is in excellent agreement with the published values of similar other ^{192}Ir HDR sources, which have similar active length of 3.5 mm. The values of radial dose function of BRIT ^{192}Ir HDR source compare well with the corresponding values of BEBIG, Flexisource, and GammaMed-12i sources due to similar active lengths and comparable phantom dimensions. The sources such as VariSource (classic, VS2000) and microSelectron (classic and v2) exhibit significant deviations in the values of radial dose function as compared to the BRIT source which is attributed to the size of water phantom employed in the simulations. The anisotropy function of BRIT ^{192}Ir HDR source is comparable with the corresponding values of microSelectron-v1 (classic) HDR source. Significant differences along source axis are observed, when compared with other ^{192}Ir HDR source models. It is proposed to utilize the Monte Carlo-calculated dose data as inputs for the indigenous development of brachytherapy treatment planning software. For clinical use, independent validation

of this Monte Carlo data generated in this work, either through experimental measurements and/or Monte Carlo simulation using a different code would be helpful in ascertaining its reliability.

Acknowledgments

The authors would like to thank Dr. D. Datta, Head, Radiological Physics & Advisory Division, Bhabha Atomic Research Centre (BARC) and Dr. Pradeepkumar K. S., Associate Director, Health, Safety and Environment Group, BARC for their encouragement and support for this work.

Financial support and sponsorship

Nil.

Conflicts of interest

There are no conflicts of interest.

References

1. Williamson JF, Li Z. Monte Carlo aided dosimetry of the microselectron pulsed and high dose-rate ^{192}Ir sources. Med Phys 1995;22:809-19.
2. Daskalov GM, Löffler E, Williamson JF. Monte Carlo-aided dosimetry of a new high dose-rate brachytherapy source. Med Phys 1998;25:2200-8.
3. Granero D, Pérez-Calatayud J, Ballester F. Monte Carlo calculation of the TG-43 dosimetric parameters of a new BEBIG Ir-192 HDR source. Radiother Oncol 2005;76:79-85.
4. Wang R, Sloboda RS. Monte Carlo dosimetry of the VariSource high dose rate ^{192}Ir source. Med Phys 1998;25:415-23.
5. Angelopoulos A, Baras P, Sakelliou L, Karaiskos P, Sandilos P. Monte Carlo dosimetry of a new ^{192}Ir high dose rate brachytherapy source. Med Phys 2000;27:2521-7.
6. Granero D, Pérez-Calatayud J, Casal E, Ballester F, Venselaar J. A dosimetric study on the Ir-192 high dose rate flexisource. Med Phys 2006;33:4578-82.
7. Ballester F, Puchades V, Lluch JL, Serrano-Andrés MA, Limami Y, Pérez-Calatayud J, *et al.* Technical note: Monte-Carlo dosimetry of the HDR 12i and Plus ^{192}Ir sources. Med Phys 2001;28:2586-91.
8. Li Z, Das RK, DeWerd LA, Ibbott GS, Meigooni AS, Pérez-Calatayud J, *et al.* Dosimetric prerequisites for routine clinical use of photon emitting brachytherapy sources with average energy higher than 50 keV. Med Phys 2007;34:37-40.
9. Perez-Calatayud J, Ballester F, Das RK, Dewerd LA, Ibbott GS, Meigooni AS, *et al.* Dose calculation for photon-emitting brachytherapy sources with average energy higher than 50 keV: Report of the AAPM and ESTRO. Med Phys 2012;39:2904-29.
10. Nath R, Anderson LL, Luxton G, Weaver KA, Williamson JF, Meigooni AS. Dosimetry of interstitial brachytherapy sources: Recommendations of the AAPM Radiation Therapy Committee Task Group No. 43. American Association of Physicists in Medicine. Med Phys 1995;22:209-34.
11. Rivard MJ, Coursey BM, DeWerd LA, Hanson WF, Huq MS, Ibbott GS, *et al.* Update of AAPM Task Group No 43 Report: A revised AAPM protocol for brachytherapy dose calculations. Med Phys 2004;31:633-74.
12. Rogers DW, Kawrakow I, Seuntjens JP, Walters BR. NRC User Codes for EGSnrc, NRC Technical Report No. PIRS-702. Ottawa, Canada: National Research Council of Canada; 2006. Available from: http://www.irs.inms.nrc.ca/inms/irs/EGSnrc/EGSnrc.html. [Last accessed on 2009 Sep 16].
13. Kawrakow I, Seuntjens JP, Rogers DW, Tessier F, Walters BR. The EGSnrc Code System: Monte Carlo Simulation of Electron and Photon Transport, NRCC Report No. PIRS-701. Ottawa, Canada: National Research Council of Canada; 2013.
14. Ballester F, Hernández C, Pérez-Calatayud J, Lliso F. Monte Carlo calculation of dose rate distributions around ^{192}Ir wires. Med Phys 1997;24:1221-8.
15. Karaiskos P, Sakelliou L, Sandilos P, Vlachas L. Limitations of the point and line source approximations for the determination of geometry factors around brachytherapy sources. Med Phys 2000;27:124-8.
16. Selvam TP, Sahoo S, Vishwakarma RS. EGSnrc-based Monte Carlo dosimetry of CSA1 and CSA2 ^{137}Cs brachytherapy source models. Med Phys 2009;36:3870-9.
17. Taylor RE, Yegin G, Rogers DW. Benchmarking brachydose: Voxel based EGSnrc Monte Carlo calculations of TG-43 dosimetry parameters. Med Phys 2007;34:445-57.
18. Hubbell JH, Seltzer SM. Tables of X-ray Mass Attenuation Coefficients and Mass Energy-Absorption Coefficients 1 keV to 20 MeV for Elements Z=1 to 92 and 48 Additional Substances of Dosimetric Interest. NIST Interagency Report No. 5632; 1995.
19. Berger MJ, Hubbell JH. XCOM, Photon Cross Sections on a Personal Computer, Report No. NBSIR 87-3597. Gaithersburg, MD: NIST; 1987.
20. Granero D, Perez-Calatayud J, Pujades-Claumarchirant MC, Ballester F, Melhus CS, Rivard MJ. Equivalent phantom sizes and shapes for brachytherapy dosimetric studies of ^{192}Ir and ^{137}Cs. Med Phys 2008;35:4872-7.